



An equivalent strain/Coffin–Manson approach to multiaxial fatigue and life prediction in superelastic Nitinol medical devices

Amanda Runciman^{a,b}, David Xu^{a,b}, Alan R. Pelton^c, Robert O. Ritchie^{a,b,*}

^a Department of Materials Science and Engineering, University of California, Berkeley, CA, USA

^b Materials Sciences Division, Lawrence Berkeley National Laboratory, CA, USA

^c Nitinol Devices and Components, Fremont, CA, USA

ARTICLE INFO

Article history:

Received 9 March 2011

Accepted 24 March 2011

Available online 30 April 2011

Keywords:

Medical devices

Nitinol

Fatigue

Life prediction

Multiaxial loads

ABSTRACT

Medical devices, particularly endovascular stents, manufactured from superelastic Nitinol, a near-equiatomic alloy of Ni and Ti, are subjected to complex mixed-mode loading conditions *in vivo*, including axial tension and compression, radial compression, pulsatile, bending and torsion. Fatigue lifetime prediction methodologies for Nitinol, however, are invariably based on uniaxial loading and thus fall short of accurately predicting the safe lifetime of stents under the complex multiaxial loading conditions experienced physiologically. While there is a considerable body of research documented on the cyclic fatigue of Nitinol in uniaxial tension or bending, there remains an almost total lack of comprehensive fatigue lifetime data for other loading conditions, such as torsion and tension/torsion. In this work, thin-walled Nitinol tubes were cycled in torsion at various mean and alternating strains to investigate the fatigue life behavior of Nitinol and results compared to equivalent fatigue data collected under uniaxial tensile/bending loads. Using these strain-life results for various loading modes and an equivalent referential (Lagrangian) strain approach, a strategy for normalizing these data is presented. Based on this strategy, a fatigue lifetime prediction model for the multiaxial loading of Nitinol is presented utilizing a modified Coffin–Manson approach where the number of cycles to failure is related to the equivalent alternating transformation strain.

Published by Elsevier Ltd.

1. Introduction

An increasing number of medical implant devices are manufactured from Nitinol, a near-equiatomic intermetallic nickel–titanium alloy, due to its unique characteristics of superelasticity and shape memory coupled with biocompatibility, large strain recovery and corrosion resistance [1]. Many of these medical devices, particularly endovascular stents, undergo tens to hundreds of millions of loading cycles in a corrosive physiological environment during their lifetime. Accordingly, to ensure their structural integrity during patient lifetimes, *in vitro* stress–life (S/N), or appropriately strain–life (ϵ/N), fatigue data are routinely determined for the alloy and combined with full component testing to develop design and life–prediction strategies for the safe use of the device.

The vast majority of stress- or strain-life fatigue data on Nitinol to support such life-prediction procedures is based on cyclic testing under uniaxial loading [2]. However, many medical devices, for example endovascular stents, are subjected to far more complex modes of loading in the body which have the potential to result in premature fractures. Recent studies have shown that arteries, particularly the superficial femoral artery (SFA), experience a dynamic combination of axial compression and extension, radial compression, bending, and torsion [3–8]. In particular, three-dimensional magnetic resonance imaging (MRI) of the SFA has revealed that this artery undergoes significant twisting of 60° ($\pm 34^\circ$) when the hip and knee are flexed under simulated walking conditions [3,6]. Despite these observations, current fatigue lifetime prediction analyses are based solely on uniaxial loading and thus may fall far short of accurately predicting the safe life of stents under these physiological multiaxial loading conditions. Specifically, ignoring modes of loading other than the regular pulsatile loads within the artery, as has been the general practice for stents up to now, has the potential for severe underestimates of safe lifetimes. Indeed, stents located in the SFA have been reported to fracture *in vivo* through the propagation of spiral cracks (termed

* Corresponding author. Department of Materials Science and Engineering, University of California, Berkeley, CA, USA. Tel.: +1 510 486 5798; fax: +1 510 643 5792.

E-mail address: roritchie@lbl.gov (R.O. Ritchie).

“spiral dissection”) [4,9]. Furthermore, studies have shown a correlation between stent fracture and patency whereby stented vessels re-occlude due *in vivo* fatigue fractures [10]. This latter phenomenon suggests that the torsional loading experienced by stents is significant and thus must be incorporated in any design and life-prediction analyses of these components.

Under uniaxial conditions, the stress- or strain-life fatigue behavior of Nitinol has been investigated for many different types of loading, including rotary bending [11,12], uniaxial fully reversed loading [13,14], and bending [15]; for a recent comprehensive review, see ref. [2]. Data are generally collected in terms of the number of cycles to failure as a function of the applied alternating and mean stresses. However, because of its superelastic behavior, where significant (superelastic) global strain can occur at essentially constant stress, as shown by the plateau in the monotonic tensile stress–strain curve (Fig. 1), expressing lifetimes for Nitinol in terms of the applied strains, rather than stresses, is far more appropriate. Additionally, it is apparent that unlike most conventional metallic materials, the amplitude of the alternating strain in Nitinol has a much more significant effect on the fatigue life than the applied mean strain, at least for mean strains below $\sim 1.5\%$ [15–20].

The most complete study on the (uniaxial) strain-life fatigue of Nitinol is due to Pelton and co-workers [15,16], who investigated diamond-shaped Nitinol samples, processed to emulate the commercial processing of Nitinol stents, which could be cycled in tension/compression by bending the diamond arms. Specifically, using finite element analysis to calibrate the stresses and strains in these test samples, where the highest strain conditions occurred on the arms of the diamond shape where the tensile and compressive stresses alternated between the bottom and the top of the arms, these authors generated a comprehensive data set for the strain-life fatigue of Nitinol under uniaxial conditions, specifically in tension/compression loading by bending.

Unlike tension/compression/bending loading, there are no corresponding comprehensive fatigue data available in the literature for the torsional fatigue loading of Nitinol, although a few studies pertain to torsional behavior under non-cyclic loads [21–25]. McNaney, Imbeni *et al.* [22,23] examined both the axial tension/compression and torsional stress–strain hysteresis behavior of the Nitinol tubing typically used to make commercial stents. These

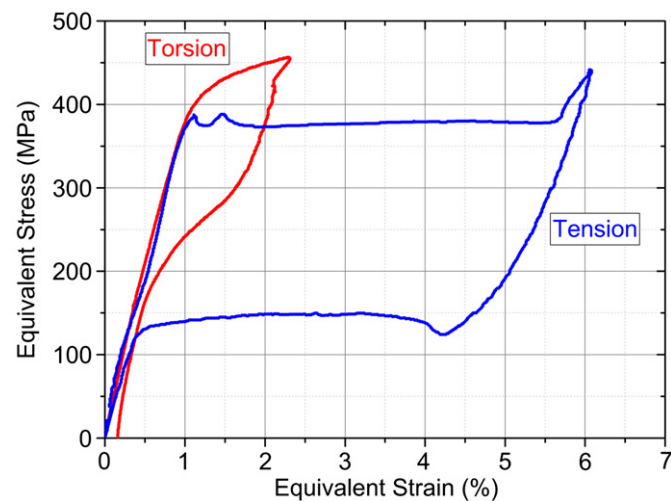


Fig. 1. Plot of the constitutive stress–strain and hysteresis behavior of superelastic austenitic Nitinol tubing loaded in axial tension vs. torsion. Although compared on the basis of the equivalent true (Cauchy) stress, $\bar{\sigma}$, as a function of the equivalent referential (Lagrangian) strain, $\bar{\epsilon}$, there is nevertheless no normalization of the torsion and tension stress–strain curves under monotonic loading. Data from Ref. [17,18].

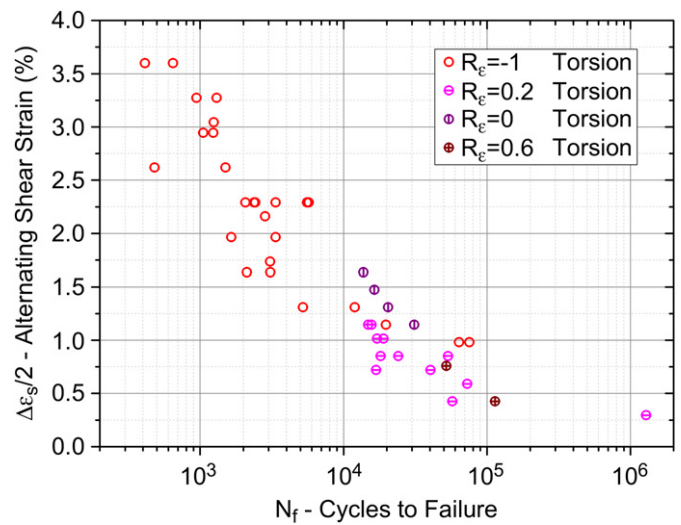


Fig. 2. Torsional fatigue ϵ/N diagram for superelastic austenitic Nitinol tubes, plotted in terms of the alternating shear strain, $\Delta\epsilon_s/2$, as a function of the number of cycles, N_f , for tests under fully reversed ($R_\epsilon = -1$) and applied mean strain ($R_\epsilon = 0, 0.2$ and 0.6) conditions.

authors measured the (non-cyclic) stress/strain behavior in tension vs. torsion and compared the resulting stress/strain hysteresis curves on the basis of the equivalent stress and equivalent strain; unlike traditional metallic materials, they found that no universal constitutive relationship in terms of the equivalent stress as a function of equivalent plastic strain existed.

In light of the MRI observations of the twisting of arteries and the current lack of information on the behavior of Nitinol alloys under torsional loads, especially the absence of S/N or ϵ/N fatigue data for torsion and/or mixed-mode loading, the current work is focused on determining the torsional strain-life fatigue curve for the superelastic Nitinol tubing used for stents, at several strain ratios of ($R_\epsilon = \epsilon_{\min}/\epsilon_{\max}$) between -1 and 0.6 , and comparing such data with existing strain-life data for a similar Nitinol alloy under tension/tension and tension/compression loading in bending over a very wide range of strain ratios from -1 to 0.99 . We further provide an approach for normalizing tension/compression/bending and torsional fatigue data in terms of the equivalent strain as a preliminary approach to developing a multiaxial design and lifetime prediction methodology based on the equivalent alternating strain for Nitinol medical devices subjected to mixed-mode fatigue loading. Based on this methodology, we propose a modified Coffin–Manson relationship for the multiaxial fatigue of superelastic Nitinol which relates the number of cycles to failure to the alternating equivalent transformation strain.

2. Materials and methods

2.1. Material

Nitinol tubing samples, with a composition of Ti, 50.8 at.% Ni ($\text{Ni}_{50.8}\text{Ti}_{49.2}$), identical to that used to manufacture endovascular stents, were received from Nitinol Devices & Components, Inc. (Fremont, CA). The NiTi tubing had an outer diameter of 3.18 mm and an inner diameter of 2.52 mm. Samples were cut to a length of 70 mm, with a gauge section precision machined to a reduced outer diameter of 3.0 mm, and then honed using abrasive flow machining to polish the outer surface of the tubing samples and remove defects caused by drawing and machining.

Samples were then heat treated to obtain an austenite finish temperature, A_f , consistent with that of commercial stents; specifically, an annealing time and temperature were used to obtain a final A_f of 16°C . The samples were tested in fatigue (in the superelastic austenitic condition) in room temperature air, resulting

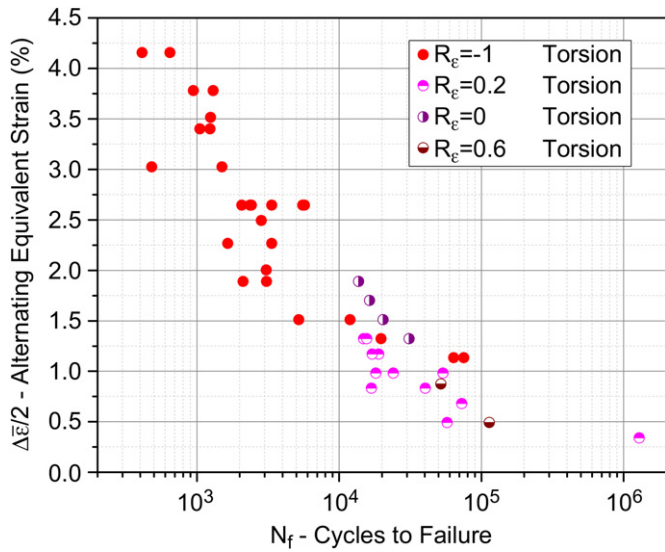


Fig. 3. Torsional fatigue ϵ/N diagram, plotted in terms of the alternating equivalent strain, $\Delta\bar{\epsilon}/2$, as a function of the number of cycles, N_f , for superelastic austenitic Nitinol tubing tested under fully reversed ($R_\epsilon = -1$) and applied mean strain ($R_\epsilon = 0, 0.2$ and 0.6) conditions.

in a $\Delta T = T - A_f$ of 9°C , representing a difference, between the testing/service temperature, T , and A_f equivalent to that with the *in vivo* operation of commercial stents [26].

Prior to testing, the samples were further polished with an $\text{HF-HNO}_3\text{-H}_2\text{O}$ etch to remove remaining oxide on both the inner and outer surfaces of the tubing. Lastly, a chemical polishing solution was introduced to the inner diameter of the tubing to ensure a smooth inner surface finish.

Additionally, to provide a comparison to the torsional fatigue results, very high mean strain ($R_\epsilon \rightarrow 1$) tension–tension data were collected on “strut” specimens, which are test devices laser machined and processed from Nitinol ($\text{Ni}_{50.8}\text{Ti}_{49.2}$) tubing, with an outer diameter of 1.07 mm and a wall thickness of 0.15 mm. These samples had an A_f temperature of $\sim 22^\circ\text{C}$ but were tested at 37°C , *i.e.*, with a ΔT of 15°C , comparable with that of the torsion tests. 15 specimens were tested, with gauge dimensions of 6 mm long, 0.30 mm wide and 0.15 mm thick.

2.2. Experimental testing

All single-cycle and torsional fatigue tests were performed using a Bose ElectroForce 3200 desktop mechanical testing system (Bose, Eden Prairie, MN) with torsional and axial testing capabilities. Samples were loaded in room temperature air in displacement-control under various torsional loading conditions using custom-designed collet grips, with collets that had a tungsten carbide coating on the inner diameter to prevent specimen slippage during torsional cyclic loading.

Fully reversed single-cycle torsional loading data were obtained at various strain levels to determine the loading/unloading hysteresis curves for the superelastic Nitinol tubing material used for the fatigue testing. With respect to the fatigue, fully reversed torsional fatigue samples were tested at a cyclic frequency of 5 Hz at equivalent strain amplitudes ranging from 1 to 4%, *i.e.*, at $R_\epsilon = -1$. Samples were tested either (i) to outright failure when the sample fully fractured into multiple pieces, (ii) when a crack formed that was sufficient to decrease the torque by 0.05 Nm, or (iii) to a maximum of 10^7 cycles (run-outs). In addition to determining the torsional strain-life curve at $R_\epsilon = -1$ with zero mean strain, the corresponding curve with a small positive mean strain, *i.e.*, at $R_\epsilon \neq -1$, was also obtained with applied equivalent mean strains and strain amplitudes ranging from 0.5 to 2% and 0.25 to 1.3%, respectively. Additional tests were also performed on a more limited basis at R_ϵ values of 0 and 0.6.

To obtain comparison data at very high strain ratios in other loading modes, tension–tension specimens were cycled out to fracture or to a maximum of 10^7 cycles at R_ϵ values between 0.88 and 0.99; results were consistent with existing Nitinol fatigue data. Fifteen specimens were fatigue tested at 9% mean strain, with alternating strain of between 0.05 and 0.6%. Uniaxial tensile tests of the struts provided relationships between displacement (mm) and strain (%). These tests were conducted in a water bath at 37°C , *i.e.*, with a ΔT of 15°C , on a Bose ElectroForce 3330 mechanical testing system.

2.3. Data analysis

Displacement and load data were collected for the single-cycle torsional tests to determine the hysteresis and constitutive behavior of the Nitinol tubes. Corresponding displacements and number of cycles to failure were measured for the fully reversed and mean strain amplitude fatigue torsional tests to create the ϵ/N curves for these conditions. Along with the sample geometry, the displacement and load data were respectively used to determine the shear stresses and shear strains applied to the samples during testing.

In order to compare the torsional hysteresis and fatigue data with previous results obtained under axial tension and compression [15,16,22,23], the shear strain values were converted to equivalent strains. The results were expressed as the equivalent true (Cauchy) stress, $\bar{\sigma}$, and the equivalent referential (Lagrangian) strain, $\bar{\epsilon}$. The data were converted by using $\bar{\sigma} = \sqrt{\sigma_t^2 + 3\sigma_s^2}$ and $\bar{\epsilon} = \sqrt{\epsilon_t^2 + 4/3\epsilon_s^2}$, where σ_t and ϵ_t are, respectively, the tensile stress and strain and σ_s and ϵ_s are, respectively, the

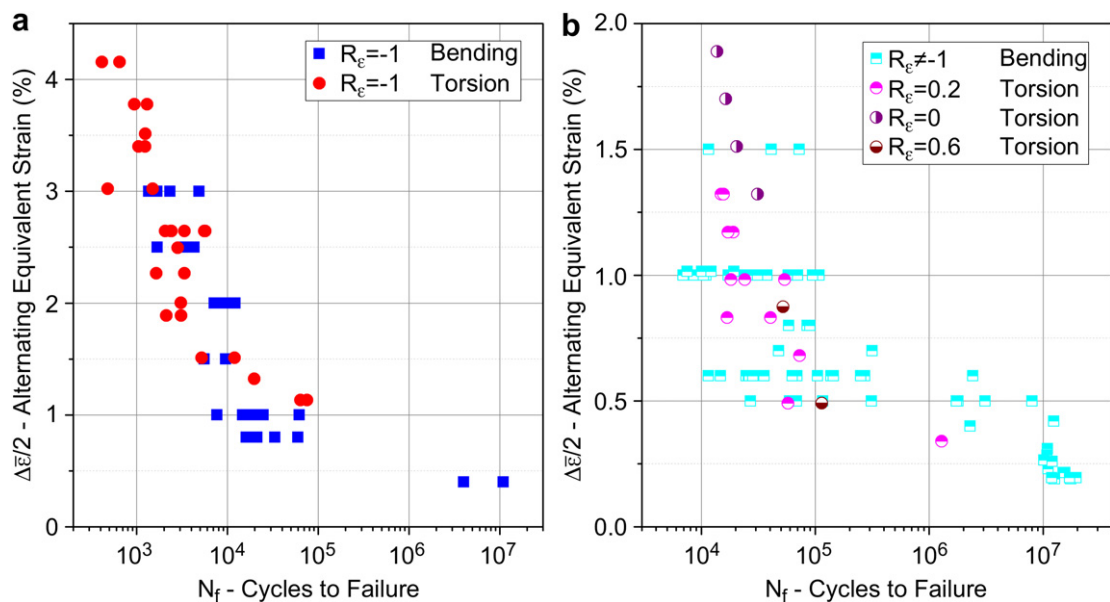


Fig. 4. Multiaxial fatigue ϵ/N diagrams plotted in terms of the alternating equivalent strain, $\Delta\bar{\epsilon}/2$, as a function of the number of cycles, N_f , for superelastic austenitic Nitinol tubing showing a comparison at lower mean strains ($-1 \leq R_\epsilon \leq 0.6$) of torsion and axial tension/compression results (a) under fully reversed ($R_\epsilon = -1$) loading and (b) with an applied mean strains ($R_\epsilon = 0, 0.2$ and 0.6). Note that data points greater than 10^7 cycles represent “run-outs”, *i.e.*, the samples did not fail.

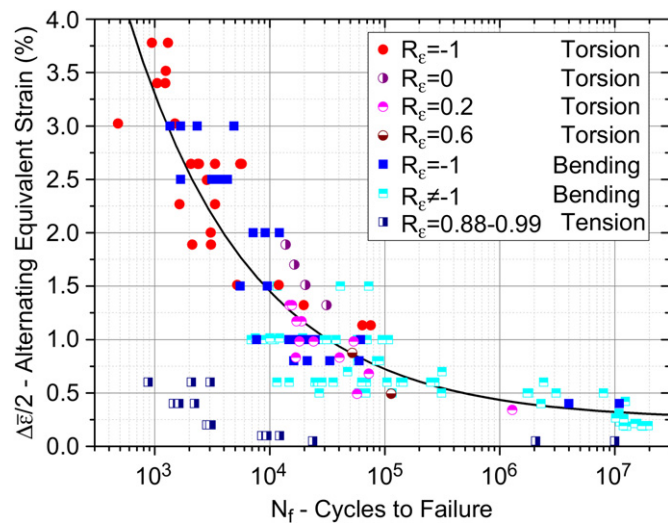


Fig. 5. Combined ε/N diagram for the multiaxial fatigue of superelastic Nitinol tubes plotted in terms of alternating equivalent strain, $\Delta\bar{\varepsilon}/2$, as a function of the number of cycles, N_f , showing normalization of multiple data sets of torsion, bending (tension/compression) and tension–tension fatigue results at multiple R_e ratios. A curve fit is shown for the lower R_e ratio results ($-1 \leq R_e \leq 0.6$) as a possible simple constitutive equation: $\Delta\bar{\varepsilon}/2 = 0.25 + 49.6N_f^{-0.4}$ for multiaxial fatigue of Nitinol at lower mean strains. This formulation does not appear to work so well for very high mean strain ($R_e \sim 0.88-0.99$) ε/N fatigue results.

shear stress and strain. For the deformation range of interest in this work, *i.e.*, strains less than 5%, the transformation strains, ε_{tr} , are defined as the total strain minus the (purely) elastic strain.

3. Results

3.1. Torsional constitutive/hysteresis behavior

Single-cycle torsional tests were conducted to determine the constitutive and hysteresis behavior of the Nitinol tubing samples to various strain levels. Such data were then compared to our previous tension vs. torsional studies on a similar composition of Nitinol tested at a similar ΔT [15,16,22,23]. Fig. 1 shows the uniaxial tension and torsional hysteresis loops plotted in terms of the equivalent stress and strain, the tensile data out to a tensile strain of 0.06, the torsional data out to a shear strain of 0.02.

3.2. Torsional fatigue strain-life behavior

The strain-life torsional ε/N curve for superelastic Nitinol, based on samples tested with fully reversed loading out to 10^6 cycles at zero mean strain ($R_e = -1$) is shown in Fig. 2 in the form of the lifetime (N_f) as a function of the applied shear strain amplitude $\Delta\varepsilon_s/2$; also plotted are the corresponding torsional data with a positive mean strain, *i.e.*, at $R_e = 0.2$. Although there is limited overlap of data, the positive mean strain ($R_e = 0, 0.2, 0.6$) results do appear to merge reasonably well with the larger number of $R_e = -1$ data points.

4. Discussion

4.1. Normalization of multiaxial behavior

The comparison in Fig. 1 of the single-cycle constitutive/hysteresis behavior of superelastic austenitic Nitinol tubing under torsion as compared to axial tension/compression loading [22,23] indicates that even when expressed in terms of the equivalent stress vs. equivalent strain, there is little to no normalization of behavior in the superelastic alloy (except in the purely elastic

range); this is in contrast to what would be expected for classical (flow theory) plasticity in a traditional (non-superelastic) metal.

Despite this lack of correlation under non-cyclic loading in superelastic Nitinol, from the perspective of providing a basis for multiaxial fatigue, the equivalent stress approach is one of two classes of multiaxial fatigue models that have been successfully used to predict lifetimes or allowable stresses under complex states of stress [e.g., 27,28]; the other class of models is based on the so-called critical plane approach [e.g., 29,30]. Equivalent stress models are an extension of the J_2 flow theory of plasticity to cyclic loading; they are essentially the cyclic version of the von Mises initial yield criterion where the normal and shear stresses associated with the fatigue loading, both alternating and mean, are expressed as an equivalent stress. These models can suffer from difficulties in defining the mean stress; moreover, from physical mechanism perspective they are fundamentally questionable as unlike continuum plasticity which is non-directional, damage in fatigue is crack formation which is highly directional and thus quite different in, for example, tension vs. shear. Despite these distractions, various versions of such equivalent stress models are in current widespread use for multiaxial fatigue. The other class of models, critical plane models [e.g., 29,30], are loosely based on physical phenomena in that fatigue cracks are assumed to form on critical planes that are a function of the normal and shear stresses and strains on that plane; normal stresses/strains are assumed to open these cracks thereby reducing any crack-surface interference whereas shear stresses/strains cause dislocation motion along slip planes leading to crack initiation and growth.

As an initial strategy for multiaxial fatigue design and life prediction in superelastic Nitinol, we propose here a relatively simple strain-based approach based on the equivalent alternating strain.¹ The basis for this is two-fold. First, a comparison of the current torsional ε/N curves for the several R_e ratios of $-1, 0, 0.2$ and 0.6 , replotted in Fig. 3 in terms of the equivalent referential (Lagrangian) strain as the equivalent strain amplitude, $\Delta\bar{\varepsilon}/2$, as a function of the number of cycles, N_f , suggests a dominant effect in Nitinol of the cyclic, as opposed to mean, strain. Although there are only limited data at two of the four R_e ratios, what is perhaps initially surprising about this comparison is how the data for the various strain ratios overlap, implying that the effect of mean strain on the torsional fatigue life of Nitinol may be relatively small. We must presume here that the large superelastic strains associated with the deformation of Nitinol make it difficult to sustain a mean strain in fatigue, akin to the relaxation of mean stresses during low-cycle fatigue [31,32] of a traditional cyclically plastically deforming metal. In addition there is an increasing volume fraction of martensite with increasing mean strain.

Second, if we compare our equivalent strain amplitude vs. number of cycles data for cyclic torsion at $R_e = -1, 1, 0.2$ and 0.6 with the comprehensive strain-life data of Pelton, and co-workers [15,16] for tension/compression loading ($-1 \leq R_e \leq 0.6$) by bending of a Nitinol with an identical composition tested at a similar ΔT , the resulting alternating equivalent strain, $\Delta\bar{\varepsilon}/2$ vs. N_f , curves display an excellent normalization (within experimental scatter) of the torsion and bending data on a single ε/N curve, for both zero (Fig. 4a) and non-zero (Fig. 4b) mean strain ($R_e \leq 0.6$).

Indeed, replotting these data on a single alternating equivalent strain vs. number of cycles, $\Delta\bar{\varepsilon}/2$ vs. N_f , strain-life diagram for Nitinol tubing displays a remarkable normalization of superelastic Nitinol

¹ Aside from the fact that the “damage” in the form of cracks is directional (as alluded to above), from a fundamental perspective, the use of an equivalent strain approach for multiaxial loading of Nitinol could also be considered questionable from the fact that the progress of the *in situ* phase transformation, which is the basis of the superelastic deformation, is also directional.

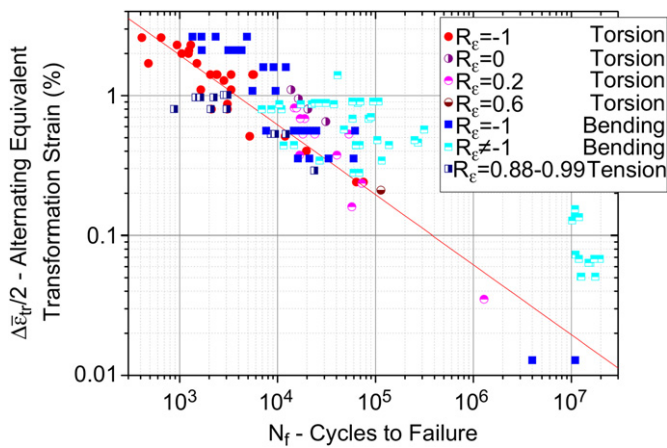


Fig. 6. A modified Coffin–Manson relationship for the multiaxial fatigue ($-1 \leq R_\epsilon \leq 0.99$) of superelastic Nitinol involving the alternating equivalent transformation strain, $\Delta\bar{\epsilon}_{tr}$, as a function of the number of cycles to failure, N_f , where $(\Delta\bar{\epsilon}_{tr}/2)N_f^{-1/2} = 61.7$. Note how this approach normalizes the ϵ/N data even for the highest mean strain results (as $R_\epsilon \rightarrow 1$).

fatigue data in both tension/compression/bending and torsion tested at lower mean strains with R_ϵ ratios less than 0.6 (Fig. 5). However, as is apparent in the Fig. 5, the normalization breaks down at the highest mean strains, as shown by the tension–tension results where the R_ϵ values assume very high values between 0.88 and 0.99.

An alternative and improved approach to displaying these data which can accommodate the high mean strain results is to incorporate a modified Coffin–Manson type equation [31,32] for the multiaxial fatigue of Nitinol utilizing the number of cycles N_f as a function of the alternating equivalent transformation strain, $\Delta\bar{\epsilon}_{tr}/2$.² Applying this notion to the current data for the torsion, bending and tension–tension fatigue of superelastic Nitinol over a wide range of strain ratios from R_ϵ values of -1 out to 0.99 now reveals a “universal” fit (Fig. 6), which can be expressed in terms of the following relationship:

$$\frac{\Delta\bar{\epsilon}_{tr}}{2} = 61.7N_f^{-1/2} \quad (1)$$

with strains expressed in %. The scatter in the data is large, akin to the fatigue of most metallic materials. However, this expression is physically appealing in mechanistic terms and is purely analogous to the traditional Coffin–Manson relationship [31,32], with essentially little to no effect of mean strain (over a wide range of strain ratios) and no indication of an apparent “fatigue limit”, but with the alternating plastic strain being replaced by the alternating equivalent transformation strain; in both cases, the relevant strain is the half-width of the fatigue (equivalent stress–strain) hysteresis loop.

Clearly both these proposed approaches for the characterization of multiaxial fatigue in superelastic Nitinol presented in Figs. 5 and 6 must be further validated with significantly more fatigue life data, specifically over a wider range of mean vs. alternating strains, out to longer lifetimes approaching 10^8 cycles or more, and ideally with other loading modes (such as internal pressure, tension plus torsion both in and out of phase, etc.). However, both approaches are relatively simple and strongly suggest that as an initial description of multiaxial fatigue in biomedical Nitinol tubing, an alternating equivalent strain-based normalization (whether computed from the total or transformation strains), with a minimal role of mean

strain, may offer a practical and workable solution. It should be noted though that the total equivalent strain formulation does not do a satisfactory job in normalizing the very high mean strain data (as $R_\epsilon \rightarrow 1$), and thus should only be used at lower mean strains ($R_\epsilon \leq 0.6$). Constitutive relationships that more fully encompass the multiaxial deformations experienced *in vivo* will also lead to higher resolution predictive finite element models, such as those used for design and analysis of Nitinol implants. Indeed, the incorporation of such multiaxial constitutive and lifetime models is essential in these numerical models for the design of safer prostheses. As nearly all Nitinol medical devices experience complex multiaxial loading conditions *in vivo* with the potential of premature fatigue failure, such equivalent strain amplitude approaches clearly show excellent promise as relatively straightforward means of predicting allowable in-service loading conditions and safe lives for implant devices subjected to mixed-mode physiological loads.

5. Conclusions

Using the stress-/strain-life (S/N or ϵ/N) methodology, a study was made of the cyclic fatigue in torsion (with and without a mean strain) of superelastic Nitinol tubing, processed in a similar fashion to the material used in many biomedical devices such as endovascular stents. Based on this study, the following conclusions can be made:

1. Although the single-cycle constitutive/hysteresis (stress vs. strain) behavior of Nitinol under torsion and axial tension loading are quite distinct and cannot be well correlated by plotting in terms of the equivalent true (Cauchy) stress, $\bar{\sigma}$, vs. the equivalent referential (Lagrangian) strain, $\bar{\epsilon}$, this approach may hold promise for normalizing cyclic fatigue data using a strain-based methodology.
2. Experimentally-measured torsional fatigue ϵ/N diagrams for Nitinol, plotted either as the shear strain amplitude, $\Delta\epsilon_s/2$, or the equivalent strain amplitude, $\Delta\bar{\epsilon}/2$, as a function of the number of cycles to failure, N_f , were found to show increased lives at lower strain amplitudes but with a minimal effect of the mean strain. Accordingly, results at a zero mean strain ($R_\epsilon = -1$) appear to fall on the same torsional ϵ/N curve as results at a positive mean stress (i.e., at $R_\epsilon = 0-0.6$), where R_ϵ is defined as the ratio of minimum to maximum strain.
3. When compared with a comprehensive set of ϵ/N fatigue data, for Nitinol of similar composition and processes, tested in bending, excellent correlation between the torsional fatigue and tension/compression (bending) fatigue was found for both zero mean strain loading ($R_\epsilon = -1$ and positive mean strain loading ($R_\epsilon = 0, 0.2$ and 0.6) when results were expressed in terms of the alternating equivalent strain, $\Delta\bar{\epsilon}/2$, as a function of the number of cycles to failure, N_f . Although working well with lower mean strain ($-1 \leq R_\epsilon \leq 0.6$) ϵ/N data, this approach did not do a satisfactory job of normalizing higher mean strain ($R_\epsilon \rightarrow 1$) data from tension/tension tests.
4. An improved approach for a multiaxial fatigue life relationship for superelastic Nitinol can be expressed in terms of a Coffin–Manson type formulation where the alternating equivalent transformation strain (or half-width of the equivalent stress-strain hysteresis loop) is related to the minus one-half power of the number of cycles to failure, $\frac{\Delta\bar{\epsilon}_{tr}}{2} \propto N_f^{-1/2}$. This approach provides a satisfactory normalization for all testing modes studied (torsion, tension/tension and bending) over the entire range of strain ratios from R_ϵ values of -1 out to 0.99.
5. Accordingly, for the design and the prediction of allowable stresses and safe lifetimes for medical devices manufactured from

² The equivalent transformation strain, $\bar{\epsilon}_{tr}$, is defined as the total equivalent strain, $\bar{\epsilon}$, minus the elastic equivalent strain, $\bar{\epsilon}_{el}$, where $\bar{\epsilon} = \bar{\epsilon}_{el} + \bar{\epsilon}_{tr}$.

superelastic Nitinol tubing and subjected to complex loading involving mixed-mode, *i.e.*, tension/compression/bending plus torsion conditions, we are advocating simple equivalent strain amplitude based approaches for multiaxial fatigue. We find that although either approach involving alternating equivalent strain vs. lifetime ε/N diagrams does an excellent job in normalizing results from different loading configurations, specifically tension, bending and torsion, at lower mean strains (*i.e.*, R_ε ratios below 0.6), the modified Coffin–Manson approach utilizing the alternating equivalent transformation strain provides a superior basis for a multiaxial fatigue law for superelastic Nitinol over a very wide range of mean strains ($-1 \leq R_\varepsilon \leq 0.99$) in torsion, tension and bending, with the alternating strain playing a dominant role compared to the mean strain.

Acknowledgments

This work was supported by initially by a grant from Nitinol Devices & Components, Inc. (Fremont, CA) and subsequently by a grant from Cordis Corporation, a subsidiary of Johnson & Johnson (Bridgewater, NJ). The authors wish to thank Brian Panganiban for his experimental assistance and Dr. Michael R. Mitchell for his invaluable advice on the torsional testing of Nitinol.

Nomenclature

Alternating shear strain, $\Delta\varepsilon_s/2$: the half amplitude of shear strain in a torsional fatigue test.

Applied shear strain, $\Delta\varepsilon_s$: the shear strain range associated with fatigue test in torsion.

Applied shear stress, $\Delta\sigma_s$: the shear stress range associated with fatigue test in torsion.

Applied tensile strain, $\Delta\varepsilon_t$: the tensile strain range associated with a fatigue test in tension.

Applied tensile stress, $\Delta\sigma_t$: the tensile stress range associated with a fatigue test in tension.

Cycles to failure, N_f : The lifetime of a fatigue sample under an applied cyclic load in cycles.

Elastic strain, ε_{el} : the range of the strain associated with only the linear elastic deformation of austenite phase in a fatigue test.

Equivalent alternating strain, $\Delta\bar{\varepsilon}/2$: the equivalent strain half amplitude of a torsional fatigue test.

Equivalent alternating transformation strain, $\Delta\bar{\varepsilon}_{tr}/2$: the half amplitude of transformation strain associated with a fatigue test.

Equivalent elastic strain, $\bar{\varepsilon}_{el}$: the equivalent strain of elastic strain, where $\bar{\varepsilon} = \bar{\varepsilon}_{el} + \bar{\varepsilon}_{tr}$.

Equivalent transformation strain, $\bar{\varepsilon}_{tr}$: the equivalent strain of transformation strain, where $\bar{\varepsilon} = \bar{\varepsilon}_{el} + \bar{\varepsilon}_{tr}$.

Equivalent strain, $\bar{\varepsilon}$: referential (Lagrangian) strain, where

$$\bar{\varepsilon} = \sqrt{\varepsilon_t^2 + 4/3\varepsilon_e^2} \text{ (sometimes known as the Mises strain).}$$

Equivalent stress, $\bar{\sigma}$: true (Cauchy) stress, where $\bar{\sigma} = \sqrt{\sigma_t^2 + 3\sigma_s^2}$ (sometimes known as the Mises stress).

Strain ratio, R_ε : The ratio between minimum and maximum strain in a fatigue test.

Temperature differential, $\Delta T = T - A_f$: representing a difference, between the testing/service temperature, T , and A_f .

Transformation strain, ε_{tr} : the range of strain associated with the transformation between the austenite to martensite phases in a fatigue test, as defined by the total strain ε minus the strain associated with elastic unloading, ε_{el} : $\varepsilon_{tr} = \varepsilon - \varepsilon_{el} = \varepsilon - \frac{\sigma}{E}$ (E is the elastic modulus).

References

- [1] Duerig TW, Pelton AR, Stoeckel D. An overview of Nitinol medical applications. *Mater Sci Eng A* 1999;273–275:146–60.
- [2] Robertson SW, Pelton AR, Ritchie RO. Mechanical fatigue and fracture of Nitinol. *Int Mater Rev*; 2011 [in review].
- [3] Cheng CP, Wilson NM, Hallett RL, Herfkens RJ, Taylor CA. In vivo MR angiographic quantification of axial and twisting deformation of the superficial femoral artery resulting from maximum hip and knee flexion. *J Vasc Interv Radiol* 2006;17:979–87.
- [4] Allie DE, Hebert CJ, Walker CM. Nitinol stent fractures in the SFA. *Endovasc Today* 2006;8:22–34.
- [5] Nikanorov A, Smouse BH, Osman K, Bialas M, Shrivastava S, Schwartz LB. Fracture of self-expanding Nitinol stents stressed in vitro under simulated intravascular conditions. *J Vasc Surg* 2008;48:435–40.
- [6] Cheng CP, Choi G, Herfkens RJ, Taylor CA. The effect of aging on deformations of the superficial femoral artery resulting from hip and knee flexion: potential clinical implications. *J Vasc Interv Radiol* 2010;21:195–202.
- [7] Ganguly A, Simons J, Schneider A, Keck B, Bennet NR, Fahrigr R. In-vitro imaging of femoral artery Nitinol stents for deformation analysis. *J Vasc Interv Radiol* 2011;22:236–43.
- [8] Ganguly A, Simons J, Schneider A, Keck B, Bennet NR, Fahrigr R, et al. In-vivo imaging of femoral artery Nitinol stents for deformation analysis. *J Vasc Interv Radiol* 2011;22:244–9.
- [9] Jaff M, Dake M, Pompa J, Ansel G, Yoder T. Standardized evaluation and reporting of stent fractures in clinical trials of noncoronary devices. *Catheter Cardiovasc Interv* 2007;70:460–2.
- [10] Scheinert D, Scheinert S, Sax J, Piorkowski C, Bräunlich S, Ulrich M, et al. Prevalence and clinical impact of stent fractures after femoropopliteal stenting. *J Am Coll Cardiol* 2005;45:312–5.
- [11] Kim YS, Miyazaki S. Fatigue properties of Ti-50.9at%Ni shape memory wires. In: Pelton AR, Hodgson D, Russell S, Duerig T, editors. SMST-97: proceedings of the second international conference on shape memory and superelastic technologies. Pacific Grove, CA: International Organization on SMST; 1997. p. 473–8.
- [12] Reinhold M, Bradley D, Bouhot R, Proft J. The influence of melt practice on final fatigue properties of superelastic NiTi wires. In: Russell SM, Pelton AR, editors. SMST-2000: proceedings of the international conference on shape memory and superelastic technologies. Pacific Grove, CA: International Organization on SMST; 2000. p. 397–403.
- [13] McNichols JL, Brookes PC, Cory JS. NiTi fatigue behavior. *J Appl Phys* 1981;52:7742–4.
- [14] Melton KN, Mercier O. Fatigue of NiTi thermoelastic martensites. *Acta Metall* 1979;27:137–44.
- [15] Pelton AR, Gong XY, Duerig TW. Fatigue testing of diamond-shaped specimens. In: Russell MS, Pelton AR, editors. SMST-2003: proceedings of the international conference on shape memory and superelastic technologies. Pacific Grove, CA: International Organization on SMST; 2003. p. 293–302.
- [16] Pelton AR, Schroeder V, Mitchell MR, Gong XY, Barney M, Robertson SW. Fatigue and durability of Nitinol stents. *J Mech Behav Biomed Mater* 2008;1:153–64.
- [17] Tabanlı RM, Simha NK, Berg BT. Mean stress effects on fatigue of NiTi. *Mater Sci Eng A* 1999;273–275:644–8.
- [18] Tolomeo D, Davidson S, Santinoranont M. Cyclic properties of superelastic Nitinol: Design implications. In: Russell MS, Pelton AR, editors. SMST-2000: proceedings of the international conference on shape memory and superelastic technologies. Pacific Grove, CA: International Organization on SMST; 2000. p. 471–7.
- [19] Kugler C, Matson D, Perry K. Non-zero mean fatigue test protocol for NiTi. In: Russell SM, Pelton AR, editors. SMST-2000: proceedings of the international conference on shape memory and superelastic technologies. Pacific Grove, CA: International Organization on SMST; 2000. p. 409–17.
- [20] Harrison WJ, Lin ZC. The study of Nitinol bending fatigue. In: Russell MS, Pelton AR, editors. SMST-2000: proceedings of the international conference on shape memory and superelastic technologies. Pacific Grove, CA: International Organization on SMST; 2000. p. 391–6.
- [21] Adler PH, Yu W, Pelton AR, Zadno R. On the tensile and torsional properties of pseudoelastic NiTi. *Scr Metall Mater* 1990;24:943–7.
- [22] Imbeni V, Mehta A, Robertson SW, Duerig TW, Pelton A, Ritchie RO. On the mechanical behavior of Nitinol under multiaxial loading conditions and in situ synchrotron X-rays. In: Russell MS, Pelton AR, editors. SMST-2003: proceedings of the international conference on shape memory and superelastic technologies. Pacific Grove, CA: International Organization on SMST; 2003. p. 267–76.
- [23] McNaney JM, Imbeni V, Jung Y, Papadopoulos P, Ritchie RO. An experimental study of the superelastic effect in a shape-memory Nitinol alloy under biaxial loading. *Mech Mater* 2003;35:969–86.
- [24] Olier P, Matheron P, Sicre J. Experimental study of torsion behavior of NiTi alloy. *J Phys IV* 2004;115:185–94.
- [25] Predki W, Klönn M, Knopik A. Cyclic torsional loading of pseudoelastic NiTi shape memory alloys: damping and fatigue failure. *Mater Sci Eng A* 2006;417:182–9.
- [26] Pelton AR, Duerig TW, Stockel D. A guide to shape memory and superelasticity in Nitinol medical devices. *Minim Invasive Ther Allied Technol* 2004;13:218–21.
- [27] Shigley JE, Mischke CR. Mechanical engineering design. 1st ed. New York: McGraw-Hill; 1989.

- [28] Manson SS, Jung K. Progress in the development of a three-dimensional fatigue theory based on the multiaxiality factor. In: *Material durability/life prediction modeling: materials for the 21st century*, ASME pressure vessel and piping, Vol. 290. Warrendale, PA: American Society for Mechanical Engineers; 1994. p. 85–93.
- [29] Smith RN, Watson P, Topper TH. A stress–strain function of the fatigue of metals. *J Mater JMLSA* 1970;5:767–78.
- [30] Brown MW, Miller KJ. A theory of fatigue under multiaxial strain conditions. *Proc Inst Mech Eng* 1973;187:745–55.
- [31] Coffin LF. A study of the effect of cyclic thermal stresses on a ductile metal. *Trans Am Soc Mech Eng* 1954;76:931–50.
- [32] Manson SS. Behavior of materials under conditions of thermal stress. In: *National advisory commission on aeronautics: report 1170*. Cleveland, OH: Lewis Flight Propulsion Laboratory; 1954.